Effect of White Mud as a Second Filler on the Mechanical and Thermal Properties of Bamboo Residue Fiber/Polyethylene Composites

Yu Xian,[a] Haidong Li,[a] Cuicui Wang,[b] Ge Wang,[a] Wenhan Ren,[a] and Haitao Cheng [a]*

The purpose of this study was to investigate the effect of white mud (WM) on mechanical and thermal properties of bamboo plastic composites (BPCs). Bamboo residue fibers (BRFs) and WM were added as the reinforcement, and high-density polyethylene (HDPE) served as the matrix. The lubricating agent and coupling agent were polyethylene wax and maleated polyethylene (MAPE), respectively. The mixture was used to manufacture BPCs using a twin-screw extruder. The crystal structure and thermal properties of BPCs were investigated by X-ray diffraction (XRD), thermogravimetric analysis (TGA), and differential scanning calorimetry (DSC). The results showed that the particle size of the WM was 700 nm to 50 μm, which are made mainly of calcium carbonate. BPCs with WM significantly increased the flexural and tensile properties, but the impact strength decreased because of the presence of WM. The flexural and tensile strength of composites with 18 wt% BPF were increased by 36.81% and 6.26%, respectively, while the flexural and tensile modulus were increased by 164.29% and 64.33%, respectively. XRD demonstrated the WM had little effect on the crystal structure of BPCs. Compared to BPCs without WM, the $T_{5\%}$ of composites with 22 wt% WM decreased by 27.9 °C. As the WM content increased, the crystallinity of the BPCs decreased initially, then increased with increasing WM content.

INTRODUCTION

Bamboo plastic composites (BPCs) are a kind of renewable and eco-friendly material that can be manufactured using bamboo, bamboo fiber, and thermoplastic resins. BPCs are used for deck boards, railings, and non-structural buildings, but now they have been expanded to the automotive and construction industries (Ratna Prasad and Rao 2011; Ramanaiah *et al*. 2012). Their mechanical functions and thermal properties are key factors that influence the application of BPCs. Due to the weak interface between bamboo fiber and polymer matrix, however, BPCs often exhibit poor mechanical properties. In order to improve the mechanical properties of BPCs, various approaches have been carried out. Some of them are concentrated on processing the bamboo fiber, such as heat treatment (Li *et al*. 2013), alkali treatment (Kumar and Kumar 2012), grafting modification (Nam *et al*. 2014), *etc*. Modifiers such as silane coupling agent (Tran *et al*. 2013) or maleic anhydride derivatized polyethylene (MAPE) compatibilizer (Mohanty and Nayak 2010) were usually added during the manufacture of BPCs. The plastics comprising the matrix are often modified by chemical treatment or radiation, *etc*. Inorganic filler also can be used to

improve the overall properties of BPCs. Mineral products such as montmorillonite (Savas and Hancer 2015), talc (Huang *et al*. 2013), and calcium carbonate (Li *et al*. 2013) have been used for this purpose. The modification approaches, as just described, generally lead to increased costs of BPCs, as well as more complicated processing technology.

In recent years, eco-environmental damage and solid residues produced by industrial activities have dramatically increased around the world. One of the most common waste disposal methods is in controlled landfills. Thus, the best way to handle these increased waste problems is to minimize the generation of solid residues or take full advantage of them as alternative raw materials whenever possible. Bamboo residue fibers (BRFs) and white mud (WM) are the solid residues generated by bamboo paper factories; BRFs are the leftover materials, or bamboo wools, which contain mostly cellulose, hemicelluloses, and lignin. Large amounts of WM can be generated during the process of alkali recovery or chemical pulping. Each ton of paper pulping produces 0.50 to 0.65 tons of WM (Liu 2009). The primary component of WM is calcium carbonate (Khunton *et al*. 2014). In the past, calcium carbonate was used as an additive in plastic (Deshmane *et al*. 2007; Garbarski and Fabijański 2013; Kuliev and Ismaiilova 2013; Frida *et al*. 2014). For example, it has been reported that fillers in polypropylene generated the following improvements: increased stiffness, strength, hardness, and melt viscosity. On the other hand, the impact strength was reduced (Jilkén *et al*. 1991; Nurdina *et al*. 2009). Venkatesan *et al*. (2014) studied organo-modified clay of montmorillonite (MMT) and high-density polyethylene (HDPE) nanocomposites. Compared to virgin HDPE, the addition of MMT nanoclay to HDPE significantly influenced the mechanical properties of the composites (Elleithy *et al*. 2010). It was also reported that the addition of nanosized calcium carbonate influences not only the mechanical properties and the creep behavior, but also the crystallinity, melting point, and rheological properties (Qi *et al*. 2013). In addition, mineral fillers can have a positive impact on the moisture resistance and mechanical properties of wood-plastic composites (WPCs) (Huuhilo *et al*. 2010). The physical and mechanical properties of WPCs hybridized with inorganic fillers have been studied, and the results showed that the best performance in mechanical strength was with kaolin and talc to a lesser extent (Gwon *et al*. 2012). The thermal properties of WPCs were also investigated with the addition of mineral fillers (Martikka *et al*. 2012).

A few studies have focused on manufacturing BPCs using the residues from bamboo papermaking. Ren and colleagues (2014) reported that bamboo pulp fibers and bamboo flour were used to obtain BPCs, and compared the mechanical and thermal properties of BPCs with differing bamboo pulp fibers content. Up to now, the utilization of WM, BRFs, and HDPE for manufacturing BPCs has no published reports. Therefore, the objectives of this study were to study the effect of WM content on the mechanical and thermal properties of BPCs.

EXPERIMENTAL

Materials

The BRFs and WM were obtained from the Chitianhua Paper Company Ltd. (Guizhou, China). High-density polyethylene with a density of 0.945 g/cm^3 (DGDK-3364), a melt flow index of 0.075 g/min (190 °C, 2.16 kg), and a tensile strength of 22.1 MPa was supplied by Zhang Mu Tou Plastic Company Ltd. (Guangzhou, China). Maleic anhydride, in the form of maleated polyethylene (MAPE) coupling agent, was also purchased from

Zhang Mu Tou Company Ltd. (Guangzhou, China). The lubricant PE-Wax was supplied by Yi-li Chemical Reagent Company (Beijing, China).

Methods

Preparation of samples

Conditions were selected on the basis of earlier research by the author group (Ren *et al*. 2014). Formulations of the components for the BPCs are illustrated in Table 1.

Table 1. Formulations of the Premix for BPCs Samples

Sample	HDPE (%)	BRFs (%)	WM (%)	MAPE (%)	PE-wax (%)
1	45	50	0	4	1
2	39	50	6	4	1
3	35	50	10	4	1
4	31	50	14	4	1
5	27	50	18	4	1
6	23	50	22	4	1

The mixtures were premixed 40 min prior to being fed through a twin-screw extruder (SJZ45/90-YF110; Kunshan Neoter Plastic Machinery Co., Ltd., China). The composites were then pulverized using a crushing machine (ZJ300; Zhangjiagang Yuanwei Machinery Co., Ltd., China), and the BPC pellets were prepared using an extruder (SJZ45/90-YF110; Kunshan Neoter Plastic Machinery Co., Ltd., China), with temperature profiles of 160, 165, 170, and 175 °C.

BRF and WM characterization

The micrographs and diameters of BRFs were analyzed using a FC300FX optical microscope (Leica Microsystems, Germany). The particle size of WM was measured using a laser particle size granularity analyzer (Mastersizer 2000, Malvern Instruments Ltd., UK).

Mechanical properties of BPCs

All samples originated from the extrusion sheet and were conditioned following the protocol ASTM D618 (2008) at 23 °C and 50% relative humidity (RH) for 88 h. The tensile and flexural tests were carried out using a Universal testing machine (Instron 5582, USA) according to the ASTM D638 (2010) and ASTM D790 (2010) protocols, respectively. The notched impact strength tests were conducted following ASTM D6110-10, using an Impact-type Test Machine (XJJ-5, Kecheng Testing Machine Co., LTD Chengde, China)

X-ray diffraction

The crystal structure of the BPCs' was analyzed using X-ray diffraction (XRD). A Philips X'Pert PRO diffractometer (PANalytical B. V., AE Almelo, Netherlands) was used to obtain the XRD patterns using Cu Ka lines (k = 1.5406 Å). The diffractograms were scanned from 5° to 35° using a scanning rate of 6° per min. X-ray diffractograms were taken on the HDPE, WM and BPCs.
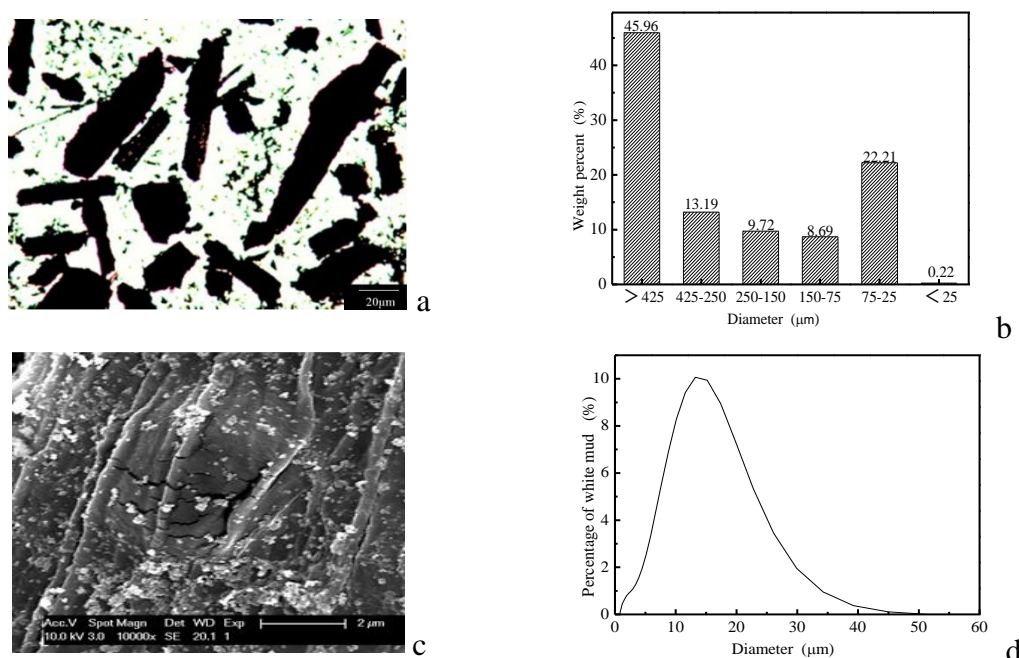
Thermal properties

Thermal properties of BPCs were examined using a thermo gravimetric analyzer Q500 (TA Instruments Inc., Delaware, USA). Each composite was heated from 35 °C to 600 °C at a rate of 10 °C per min. The thermal decomposition temperature of the composites was examined under a nitrogen atmosphere. A differential scanning calorimeter apparatus (DSC Q100, TA Instrument Inc., Delaware, USA) was used in investigating the crystallization process of the BPCs. All measurements were carried out at room temperature. Five milligrams of the composites sample were weighed in an aluminum pan and placed in the cell. The nitrogen flow rate was 60 mL per min. The samples were cooled to -20 °C for 5 min, heated from -20 °C to 180 °C at a constant rate of 10 °C per min, then cooled to -20 °C at the same rate, after 2 min, to heat up to 180 °C at a rate of 10 °C per min. The heat flow curve was recorded as a function of temperature.

RESULTS AND DISCUSSION

The BRFs and WM

The BRFs and WM distributions are shown in Fig. 1. The morphology and diameter of BRFs were measured using an FC300FX optical microscope under 50X magnification (Fig. 1a). Figure 1a shows that the particle sizes of BRFs were cylindrical with short and thick fibers, which has a small aspect ratio. This may help to explain the weak dispersivity of BRFs in HDPE. The BRFs sizes ranged from 75 to 425 μm, as shown in Fig. 1b. Figure 1c shows scanning electron microscope pictures of WM. The diagram in Fig. 2d reflects the WM size distribution. There was a large range in the particle size of the WM (700 nm to 50 μm), with a mean diameter of 12.125 μm. The WM was hybridized with micro/nano particles, and the diameter was concentrated in the range of 10 to 20 μm (Fig. 1d).

Fig. 1. Physical properties of BRF and WM. (a) optical micrograph of BRF, (b) particle size of BRF, (c) SEM of WM, and (d) particle size of WM

bioresources.com

The chemical composition of the WM and BRF are presented in Tables 2 and 3. The primary components of BRF were holocellulose and lignin. Calcium carbonate was a major component of WM (87.97%).

Table 2. Chemical Composition of BRF

| Water (wt%)	Ash (wt%)	Benzyl alcohol extract (wt%)	Holocellulose (wt%)	Lignin (wt%)
7.42	4.80	1.36	67.50	26.66

Table 3. Chemical Composition of WM

$CaCO_3$ (wt%)	CaO (wt%)	SiO_2 (wt%)	Fe_2O_3 (wt%)	NaOH (wt%)	Acid-insoluble (wt%)	Other (wt%)
87.97	1.07	2.82	0.3	0.7	1.76	3.4

Mechanical Properties

Flexural properties

Figure 2a shows that as the WM content was increased, the flexural modulus of the composites increased initially, and then they decreased. When the WM proportion was increased from 0 to 18 wt%, the BPCs' flexural modulus and strength increased as WM content increased. In accordance with the rule of mixtures, the stiffness of WM was greater than that of HDPE. Such results occurred because of the WM in BPCs, which restricted the motion of HDPE chains; therefore, the stiffness of BPCs was increased. Similar cases have been reported in other experiments (Yasmin and Daniel 2004).
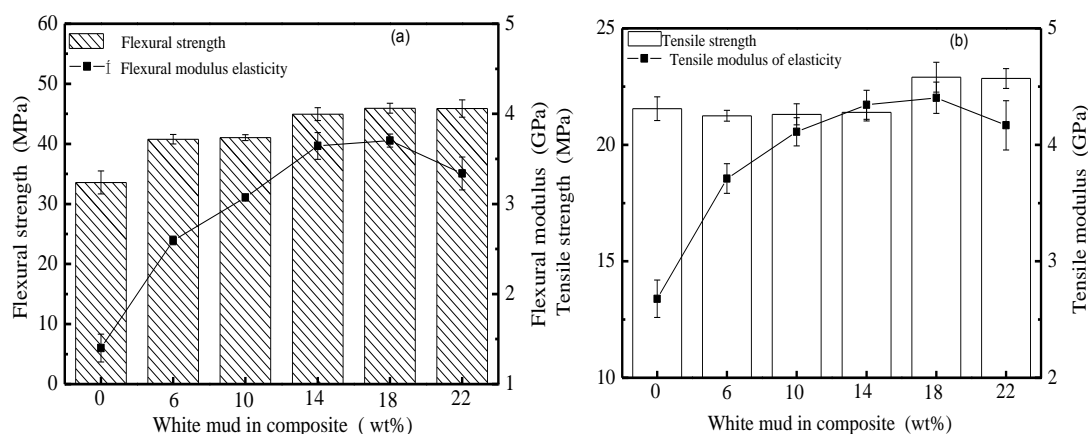
Fig. 2. Mechanical properties of BPCs: (a) flexural properties and (b) tensile properties

When the proportion of WM was increased to 18 wt%, the flexural strength and modulus of BPCs reached maximum. The flexural strength and modulus of BPCs including 18 wt% WM exhibited an improvement 36.81% and 164.29% compared to those of BPCs without WM, respectively. The flexural modulus of composites including 22 wt% WM decreased slightly compared to 18 wt% WM. Similar results were published by Ding *et al.* (2005) and Sun *et al.* (2010). This reduction of modulus was attributed to the fact that the WM are made mainly of calcium carbonate with lower molecular weight. As a result, the molecular forces between the WM, BRFs and matrix (HDPE) were too small to cross-

linking. Therefore, the WM, BRFs, and HDPE were only mechanical mixture, and the internal molecular forces of BPCs were weakened (Sun *et al*. 2010). That means the forces were unable to be transferred efficiently, which in turn reduced the mechanical stress in the transfer from the matrix to the BRFs. Consequently, the flexural modulus decreased. The flexural strength of BPCs increased to 45.94 MPa when WM content was 18 wt%, which may be attributed to the fact that the particle size of WM was less than of BRFs. The micro/nano WM particles could fill the gap of the BRF effectively, the BPCs became compacted and the homogenous dispersion of the WM in the BPCs (Sun *et al*. 2010), which in turn increased the flexural strength of the BPCs.

Tensile properties

Adding WM to the composites at different proportions improved the tensile properties of BPCs (Fig. 2b). Similar to the flexural properties, the tensile modulus of BPCs also increased initially, and then they decreased. This was attributed to the fact that the WM restricted the motion of the HDPE polymer chains and decreased the deformation capacity of the matrix in the elastic zone. The results showed that for the 18 wt% WM in composites, the maximum tensile modulus and strength were 4.40 GPa and 22.9 MPa, respectively. Compared to composites without WM, the tensile modulus and strength of composites were 64.33% and 6.26% higher than those of composites without WM, respectively. These results were expected and are in agreement with previous reports (Yasmin and Daniel 2004; Ding *et al*. 2005; Sun *et al*. 2010). The tensile modulus of composites with 22 wt% WM were worse than those of the composites with 18 wt% WM. The results indicated that when the WM content was more than 18 wt% in BPCs, the HDPE could not coat the WM completely, which led to increased stress concentration. Therefore the tensile modulus decreased (Yasmin and Daniel 2004).

SEM analysis

Figure 3 shows SEM micrographs of tensile fracture surface with different WM content in BPCs. From Fig. 3a, it can be observed by SEM that BRFs had smooth surfaces, and without adhesion of WM.
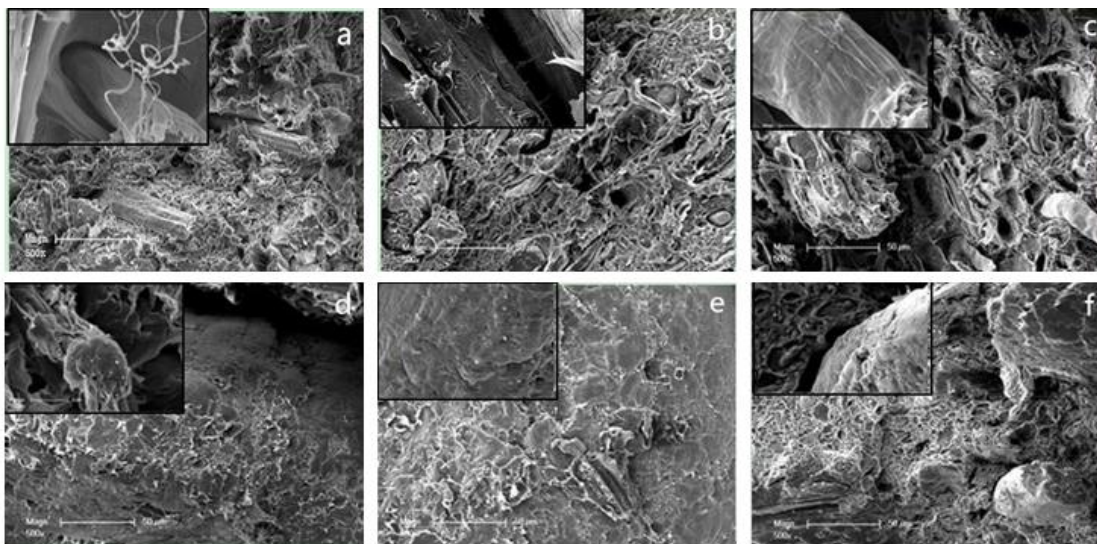

Fig. 3. Fracture surface of BPCs: (a) 0%, (b) 6%, (c) 10%, (d) 14%, (e) 18%, and (f) 22%

Figure 3 also shows that the void space existed between the BRFs and HDPE. The load did not transfer effectively from HDPE to BRFs under tensile force. So the HDPE could not coat the fiber completely, which resulted in poor tensile properties. White crazing was observed, and WM with adhesion of BRFs can be seen in Fig. 4(b-e) in the top left corner. On the other hand, because an excess of WM leads to an increased agglomeration tendency of the filler, the contact area between BRFs and HDPE was reduced and some holes were present in the tensile fracture surface of BPCs with 22 wt% WM (Figure 4f). These were consistent with the flexural and tensile properties.

Impact strength

The notched impact strengths of BPCs are shown in Fig. 4. The impact strength was strongly dependent on the proportion of WM. BPCs without WM showed the highest impact resistance. For example, the impact strength dropped to 4.03 kJ/m^2 with 18 wt% WM filled BPCs. BPCs with WM demonstrated a decrease in impact strength. This is due to the fact that the micron-WM only filled in the BRFs or tiny spaces of BRFs and HDPE, yet they were profoundly incompatible. The poor compatibility between the WM and HDPE led to unstable interfacial adhesions, such that cracks tended to grow and spread. When the impact force hit the BPCs, the BPCs absorbed less and less impact energy as the WM increased (Shi *et al*. 2013). Besides, as the WM increased in the composites, correspondingly, the amount of flexible and tougher HDPE was reduced (Wang and Yang 2009), which did not absorb enough energy. Therefore, the impact strength decreased rapidly as the content of WM was increased.
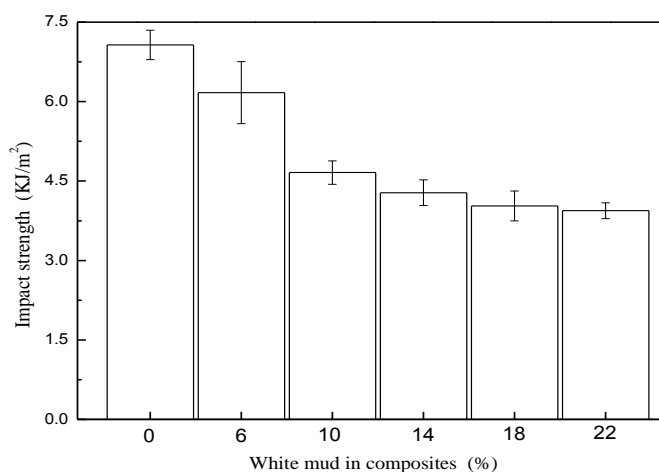
Fig. 4. Effects of WM content on the impact strength of BPCs

X-ray diffraction

Figure 5 shows the X-ray diffractogram for BPCs containing virgin WM and virgin HDPE. In virgin HDPE, the diffraction peaks were observed at 2θ Braggs angles of 21.6° and 24.0° (Chen and Yan 2013), corresponding to diffraction planes of 110 and 200, whereas WM showed an intense peak at approximately 29.4° (Tang *et al*. 2007), which was confirmed by the calcium carbonate crystal structure of 110. Apparently, apart from those of the pure substances, no new diffraction peaks were observed in the diffraction pattern of the composites. In other words, all composites showed the same XRD patterns with varying peak intensity in proportion to the weight fraction of the additives. The absence of new diffraction peaks indicated that the presence of WM had little effect on the crystal structure of HDPE. However, after adding WM, the crystallization peak strength of

bioresources.com

HDPE weakened and tended to disappear (Deshmukh *et al*. 2010). This indicated that the crystal integrity of HDPE was affected by the content of WM; the crystal integrity of the HDPE molecular chains was destroyed as WM content increased. The motions of HDPE molecular chains were limited in the BPCs. Therefore, the crystal growth of HDPE was restricted, corresponding to the peak intensity weakened.
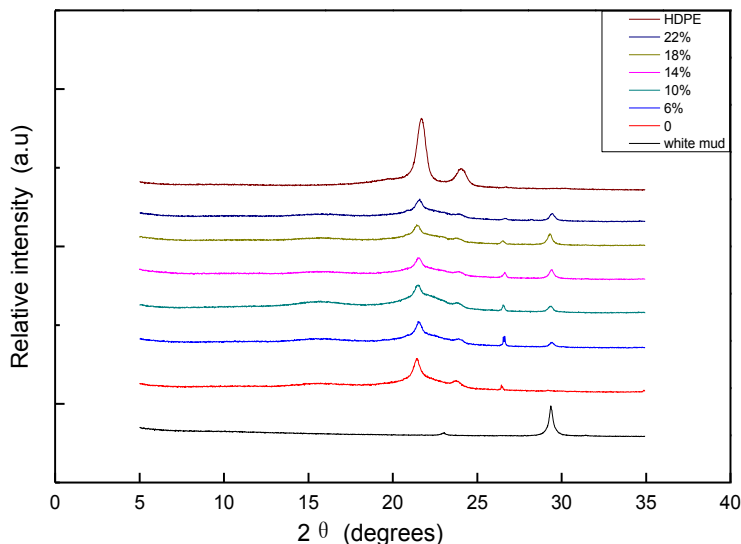

Fig. 5. Effect of varying WM content on XRD of BPCs

Thermal Properties

Thermogravimetry

      Thermo gravimetric analysis (TGA) was used to study the thermal stability and degradation of the BPCs. The TGA and DTG curves of the composites are represented in Fig. 6. The thermal degradation of all samples occurred within the programmed temperature range of 0 to 600 °C. Overall, the TGA curves for the BPCs showed two decomposition steps; the first shoulder peak in the temperature range from 300 to 400 °C indicated the degradation of cellulose, hemicelluloses, and lignin from BRFs, and the second shoulder in the range of 400 to 500 °C suggested HDPE degradation (Mengeloglu and Kabakci 2008).
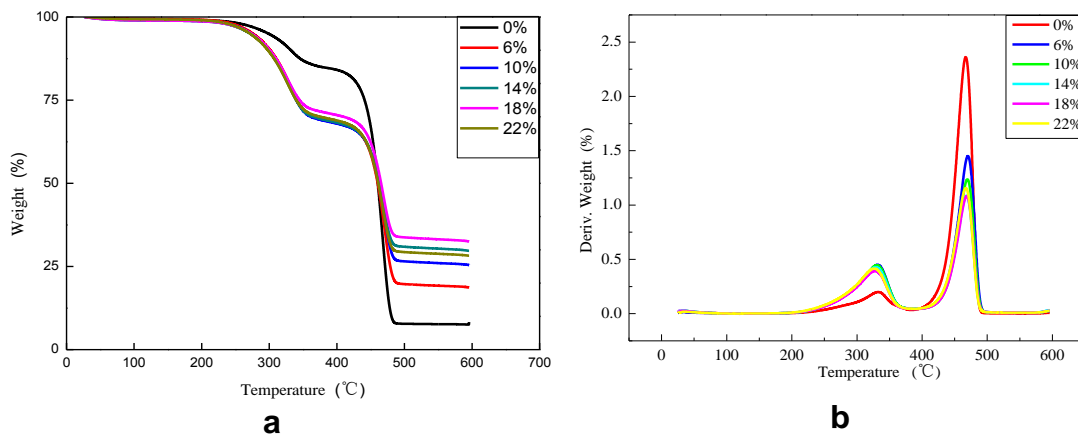

Fig. 6. Thermogravimetric curves of BPCs: (a) TGA and (b) DTG

The thermal degradation of cellulose can occur because of the cleavage of the glycoside linkage by trans glycosylation and scission of -CO and C-C bonds (Ibrahim *et al*. 2003; Nurfatimah *et al*. 2015). These results were similar to those reported by Nourbakhsh *et al*. (2010).

Table 4 shows that the initial decomposition temperature ($T_{5\%}$) decreased with increasing WM content. Compared to BPCs without WM, the $T_{5\%}$ of composites with 22 wt% WM decreased by 27.9 °C. Based on these results it is clear that the thermal stability and decomposition temperature can be affected by the presence of WM in BPCs. The fact that the degradation temperature of the composites decreased also indicated that there was poor compatibility between the WM, BRF, and HDPE. The first peak temperature (T_1) fell slightly initially, and then the curve rose slightly, whereas the second peak temperature (T_2) was irregular with the varying of WM. The WM ratio increased, but the content of HDPE was reduced. In other words, the lesser amount of HDPE was not able to coat the BRFs completely. Therefore, the thermal stability of the BPCs was influenced. These results are in agreement with previous reports (Ren *et al*. 2014). The ultimate char residue increased by 33.55% in the BPCs with 18 wt% WM composition. The reason may be that the degradation temperature of WM was controlled at 580 to 700 °C; however, it was influenced by the WM content in the composites. When the WM content reached 22 wt%, composites were easier to agglomerate and showed poor compatibility between the WM, BRF, and HDPE matrixes. For this reason, the composites were more likely to burn, reducing the ultimate char residue (Li *et al*. 2014).

Table 4. Summary of $T_{5\%}$, T_1, T_2, and Char Residue for the BPCs

WM (%)	$T_{5\%}$ (°C)	T_1 (°C)	T_2 (°C)	Char residue at 550 °C (%)
0	298.76	332.81	467.06	7.56
6	274.33	331.73	469.84	19.22
10	273.45	329.26	469.84	22.83
14	271.62	328.81	467.60	28.98
18	271.29	327.91	467.15	33.55
22	270.86	328.81	471.04	28.29

Differential scanning calorimetry

Differential scanning calorimetry (DSC) measurements were carried out to determine the melting behaviour of the BPCs. The data obtained from the DSC curves using the initial melting temperature (T_{onset}), peak melting temperature (T_m), the heat of crystallization (ΔH_m), and the percent crystallinity (X_c) are shown in Table 5. X_c of HDPE in BPCs was determined by Deshmukh *et al*. (2010) using the equation,

$$X_c\ (\%) = \Delta H_m \times 100/[\Delta H_f * W)] \tag{1}$$

where ΔH_f is the heat of fusion for 100% HDPE, ΔH_m is the heat of crystallization, and W is the mass fraction of HDPE in the composites.

Data from Table 5 show that the T_{onset} and T_m of the WM composites were slightly improved compared to composites without WM. As the WM content increased, the T_{onset} of composites increased from 100.58 °C to 107.57 °C. A possible explanation for this was that a small amount of WM acted as a nucleating agent during the crystallization of HDPE, such that the activation energy of HDPE was reduced (Shi *et al*. 2013). The crystallinity of BPCs decreased with lower WM content (14 wt%), indicating the presence of a small

amount of WM that adsorbed in the cracks in the BRFs. The BRFs hindered the overall extent of HDPE crystallization. As the WM content from 14 wt% to 22 wt%, the crystallization of the composites was increased; this may be because a small amount of WM acted as a nucleating agent during the crystallization of composites (Ma *et al*. 2002). The WM may have embedded in the HDPE molecules segments, and some WM molecules were immobilized in the HDPE. These immobilized molecules contributed to the crystallization process of HDPE. Therefore, the crystallization of HDPE molecules could occur at a higher temperature. Some similar results have been reported by Shi *et al*. (2013) and Colom *et al.* (2000). However the crystallinity of the composites decreased initially, and then they increased.

Table 5. Summary of T_{onset}, T_c, T_m, $\triangle H_m$, and X_c of BPCs

WM (%)	Crystallize		Secondary Scan			
	T_{onset} (°C)	T_c (°C)	T_{onset} (°C)	T_m (°C)	$\triangle H_m$ (J/g)	X_c (%)
0	117.47	116.23	100.58	127.37	95.09	66.33
6	117.29	116.48	106.87	126.74	50.73	40.21
10	117.31	116.27	105.82	126.53	44.64	38.92
14	117.39	116.24	106.54	126.46	37.44	36.27
18	117.53	116.30	107.40	126.52	36.74	40.04
22	117.50	116.28	107.57	126.70	39.88	49.68

CONCLUSIONS

1. The morphology of bamboo residue fibers (BRFs) is generally cylindrical and short, meaning that the BRFs had a small aspect ratio. The major component was holocellulose. The BRFs sizes ranged from 75 to 425 μm. The content of calcium carbonate was up to 87.97% in WM, which was a major component. The WM exhibited a wide distribution in diameter, from 25 to 425 μm. The mean diameter of the WM was 12.125 μm.

2. The flexural and tensile properties of BPCs were improved by WM as a reinforcing phase. When the WM content reached 18 wt%, both the mechanical modulus and strength were optimal. But the impact strength of BPCs decreased.

3. After adding WM to the BPCs, the crystallization peak strength of HDPE weakened and tended to disappeared. The WM had little effect on the crystal structure of HDPE, and no new diffraction peaks appeared in BPCs. Thermal studies showed that the initial decomposition temperature ($T_{5\%}$) of BPCs decreased as the WM content increased, but the ultimate char residue increased. With increasing WM content, the crystallinity of the BPCs decreased initially and then they increased.

ACKNOWLEDGMENTS

REFERENCES CITED

ASTM D618 (2008). "Standard practice for conditioning plastics for testing," ASTM International, West Conshohocken, PA.

ASTM D638 (2010). "Standard test method for tensile properties of plastics," ASTM International, West Conshohocken, PA.

ASTM D790 (2010). "Standard test method for flexural properties of unreinforced and reinforced plastics and electrical insulation materials," ASTM International, West Conshohocken, PA.

ASTM D6110 (2010). "Standard test method for determining the charpy impact resistance of notched specimens of plastics," ASTM International, West Conshohocken, PA.

Chen, J. M., and Yan, N. (2013). "Crystallization behavior of organo-nanoclay treated and untreated kraft fiber–HDPE composites," *Composites Part B: Engineering* 54, 180-187. DOI: 10.1016/j.compositesb.2013.05.011

Colom, X., Canavate, J., Pages P., Saurina, J., and Carrasco, F. (2000). "Changes in crystallinity of the HDPE matrix in composites with cellulosic fiber using DSC and FTIR," *Journal of Reinforced Plastics and Composites* 19(10), 818-830. DOI: 10.1106/8RMN-D1HE-75V1-7LN0

Deshmane, C., Yuan, Q., and Misra, R. D. K. (2007). "On the fracture characteristics of impact tested high density polyethylene–calcium carbonate nanocomposites," *Materials Science and Engineering A-Structural Materials Properties Microstructure and Processing* 452, 592-601. DOI: 10.1016/j.msea.2006.11.059

Deshmukh, G. S., Pathak, S. U., Peshwe, D. R., and Ekhe, J. D. (2010). "Effect of uncoated calcium carbonate and stearic acid coated calcium carbonate on mechanical, thermal and structural properties of poly(butylene terephthalate) (PBT)/calcium carbonate composites," *Bulletin of Materials Science* 3(33), 277-284. DOI: 10.1007/s12034-010-0043-7

Ding, Y. S., Geng, H. G., and Wang, S. S. (2005). "Investigation on crystallinity and morphology of ultrafine talc-filled polypropylene composites and their influence on its mechanical properties," *Polymer Material Science and Engineering* 21(5), 90-93.

Elleithy, R. H., Ali, I., Ali, M. A., and Al-Zahrani, S. M. (2010). "High density polyethylene/micro calcium carbonate composites: A study of the morphological, thermal, and viscoelastic properties," *Journal of Applied Polymer Science* 117(4), 2413-2421. DOI: 10.1002/app.32142

Frida, E., Bukit, N., and Zebua, F. (2014). "Analysis mechanics and thermal composites thermoplastic high density polyethylene with zeolite modification filler," *Chemistry and Materials Research* 3(6), 126-134.

Garbarski, J., and Fabijański, M. (2013). "The mechanical properties of a mixture of high density polyethylene and calcium carbonate dedicated for packaging," *Advances in Manufacturing Science and Technology* 37(2), 91-96.

Gwon, J. G., Lee, S.Y., Chun, S. J., Doh, G. H., and Kim, J. H. (2012). "Physical and mechanical properties of wood–plastic composites hybridized with inorganic fillers," *Journal of Composite Materials* 3(46), 301-309.DOI:10.117/0021998311413690

Huang, R. Z. Kim, B. J., Lee, S. Y., Zhang, Y., and Wu, Q. L. (2013). "Co-extruded wood-plastic composites with talc-filled shells: Morphology, mechanical, and thermal expansion performance," *BioResources* 8(2), 2283-2299. DOI: 10.15376/biores.8.2.2283-2299

Huuhilo, T., Martikka, O., Butylina, S., and Karki, T. (2010). "Impact of mineral fillers to the moisture resistance of wood-plastic composites," *Baltic Forestry* 16(1), 126-131.

Ibrahim, N. A., Yunus, W. M. Z. W., Abu-Ilaiwi, F. A., Ab Rahman, M. Z., Bin Ahmad, M., and Dahlan, K. Z. M. (2003). "Graft copolymerization of methyl methacrylate onto oil palm empty fruit bunch using H_2O_2/Fe^{2+} as an initiator," *Journal of Applied Polymer Science* 89(8), 2233-2238. DOI: 10.1002/app.12467

Jilkén, L., Malhammar, G., and Seldén, R. (1991). "The effect of mineral fillers on impact and tensile properties of polypropylene," *Polymer Testing* 10(5), 329-344. DOI: 10.1016/0142-9418(91)90011-L

Khunton, S., Nilpairach, S., and Sangsuk, S. (2014). "Using lime mud waste from pulp mill as an additive in brick clay," *Key Engineering Materials* 608, 3-7. DOI: 10.4028/www.scientific.net/KEM.608.3

Kuliev, M. M., and Ismaiilova, R. S. (2013). "The effect of an inorganic filler on the properties of high-density polyethylene," *International Polymer Science and Technology* 8(40), 33-37.

Kumar, V., and Kumar, R. (2012). "Dielectric and mechanical properties of alkali- and silane-treated bamboo-epoxy nanocomposites," *Journal of Composite Materials* 46(24), 3089-3101. DOI: 10.1177/0021998311435831

Li, P., Kim, B. J., Wang, Q. W., and Wu, Q.L. (2013). "Experimental and numerical analysis of the sound insulation property of wood plastic composites (WPCs) filled with precipitated $CaCO_3$," *Holzforschung* 67(3), 301-306. DOI: 10.1515/hf-2012-0093

Li, X., Lei, B., Lin, Z. D., Huang, L. H., Tan, S. Z., and Cai, X. (2014). "The utilization of bamboo charcoal enhances wood plastic composites with excellent mechanical and thermal properties," *Materials & Design* 53, 419-424. DOI: 10.1016/j.matdes.2013.07.028

Liu, S. J. (2009). *Study on Pulping Lime Mud and PVC Foamed Composite*, M.S. thesis, Fujian Agriculture and Forestry University, Fuzhou, China.

Li, Y. J., Du, L. X., Kai, C., Huang, R. Z., and Wu, Q. L. (2013). "Bamboo and high density polyethylene composite with heat-treated bamboo fiber: Thermal decomposition properties," *BioResources* 8(1), 900-912. DOI: 10.15376/biores.8.1.900-912

Ma, J. S., Zhang, S. M., Qi, Z. N., Li, G., and Hu, Y. L. (2012). "Crystallization behaviors of polypropylene/montmorillonite nanocomposites," *Journal of Applied Polymer Science* 83(9), 1978-1985. DOI: 10.1002/app.10127

Martikka, O., Huuhilo, T., Butylina, S., and Krki, T. (2012). "The effect of mineral fillers on the thermal properties of wood-plastic composites," *Wood Material Science and Engineering* 7(2), 107-114. DOI: 10.1080/17480272.2012.663408

Mengeloglu, F., and Kabakci, A. (2008). "Determination of thermal properties and morphology of eucalyptus wood residue filled high density polyethylene composites,"

International Journal of Molecular Sciences 2(9), 107-119. DOI: 10.3390/ijms9020107

Mohanty, S., and Nayak, S. K. (2010). "Short bamboo fiber-reinforced HDPE composites: Influence of fiber content and modification on strength of the composite," *Journal of Reinforced Plastics and Composites* 29(14), 2199-2210. DOI: 10.1177/0731684409345618

Nam, G., Wakamoto, N., Okubo, K., and Fujii, T. (2014). "Study of maleic anhydride grafted polypropylene effect on resin impregnated bamboo fiber polypropylene composites," *Agricultural Sciences* 5(13), 1322-1328. DOI: 10.4236/as.2014.513141

Nourbakhsh, A., Ashori, A., Ziaei Tabari, H., and Rezaei, F. (2010). "Mechanical and thermo-chemical properties of wood-flour/polypropylene blends," *Polymer Bulletin* 65(7), 691-700. DOI: 10.1007/s00289-010-0288-8

Nurdina, A. K., Mariatti, M. and Samayamutthirian, P. (2009). "Effect of single-mineral filler and hybrid-mineral filler additives on the properties of polypropylene composites," *Journal of Vinyl & Additive Technology* 15(1), 20-28. DOI: 10.1002/vnl.20173

Prasad, A. V. R., and Rao, K. M. (2011). "Mechanical properties of natural fibre reinforced polyester composites: Jowar, sisal and bamboo," *Materials & Design* 32(8-9), 4658-4663. DOI: 10.1016/j.matdes.2011.03.015

Qi, F. W., Luo, X. G., Lin, X. Y., and Zhang, S. Z. (2013). "Effect of $CaCO_3$ particle size and size distribution on rheological and mechanical properties of polyethylene," *Resources and Sustainable Development*, Pts. 1-4, 734-737, 2252-2255. DOI: 10.4028/www.scientific.net/AMR.734-737.2252

Ramanaiah, K., Prasad, A. V. R., and Reddy, K. H. C. (2012). "Thermal and mechanical properties of waste grass broom fiber-reinforced polyester composites," *Materials & Design* 40, 103-108. DOI: 10.1016/j.matdes.2012.03.034

Ren, W. H., Zhang, D., Wang, G., and Cheng, H. T. (2014). "Mechanical and thermal properties of bamboo pulp fiber reinforced polyethylene composites," *BioResources* 9(3), 4117-4127. DOI: 10.15376/biores.9.3.4117-4127

Savas, L. A., and Hancer, M. (2015). "Montmorillonite reinforced polymer nanocomposite antibacterial film," *Applied Clay Science* 108, 40-44. DOI:10.1016/j.clay.2015.02.021

Shi, X. B., Wang, J. L., Cai, X. P., and Zhang, S. (2013). "Role of calcium carbonate morphology on thermal and mechanical properties of HDPE," *Plastics, Rubber and Composites* 7(42), 302-307. DOI: 10.1179/1743289813Y.0000000051

Sun, X. Q., Li, Q. Y., Huang, P. P., and Zheng, Y. C. (2010). "The influence of filler on bending property of wood-plastic composite," *Journal of Qingdao Technological University* 31(2), 28-31.

Tang, Y. J., Li, Y. M., and Hu, D. W. (2007). "Modification surface structure and rheological behavior of nanosized $CaCO_3$," *Acta Chimica Sinica* 20(65), 2291-2298.

Tran, D. T., Nguyen, D. M., Thuc, C. N. H., and Dang, T. T. (2013). "Effect of coupling agents on the properties of bamboo fiber-reinforced unsaturated polyester resin composites," *Composite Interfaces* 20(5), 343-353. DOI: 10.1080/15685543.2013.806100

Venkatesan, N. G. B., Pazhanivel, B. K., and Poyyathappan, K. (2014). "Reinforcing effect of montmorillonite nanoclay on mechanical properties of high density polyethylene nanocomposites," *Applied Mechanics and Materials* 591, 60-63. DOI: 10.4028/www.scientific.net/AMM.591.60

Wang, J. Y., and Yang, Q. B. (2009). "Experimental study on ductility and toughness of HDPE pipe concrete," *Journal of Building Materials* 12(4), 394-397.

Yasmin, A., and Daniel, I. M. (2004). "Mechanical and thermal properties of graphite platelet/epoxy composites," *Polymer* 45(24), 8211-8219. DOI: 10.1016/j.polymer.2004.09.054